

Concentration dependence of the Flory-Huggins interaction parameter in aqueous solutions of capped PEO chains

M. I. Chaudhari, L. R. Pratt

Department of Chemical and Biomolecular Engineering, Tulane University, New Orleans, LA 70118

M. E. Paulaitis

*Department of Chemical and Biomolecular Engineering,
The Ohio State University, Columbus, OH 43210*

(Dated: July 16, 2021)

The dependence on volume fraction φ of the Flory-Huggins $\chi_{wp}(\varphi)$ describing the free energy of mixing of polymers in water is obtained by exploiting the connection of $\chi_{wp}(\varphi)$ to the chemical potential of the water, for which quasi-chemical theory is satisfactory. We test this theoretical approach with simulation data for aqueous solutions of capped PEO oligomers. For $\text{CH}_3(\text{CH}_2\text{-O-CH}_2)_m\text{CH}_3$ ($m=11$), $\chi_{wp}(\varphi)$ depends strongly on φ , consistent with experiment. These results identify coexisting water-rich and water-poor solutions at $T = 300$ K and $p = 1$ atm. Direct observation of the coexistence of these two solutions on simulation time scales supports that prediction for the system studied. This approach directly provides the osmotic pressures. The osmotic second virial coefficient for these chains is positive, reflecting repulsive interactions between the chains in the water, a *good* solvent for these chains.

I. INTRODUCTION

A classic element of polymer solution physics, the Flory-Huggins (FH) model,^{1,2}

$$\frac{\beta\Delta G_{\text{mix}}}{n_w + Mn_p} = \varphi \ln \varphi + \frac{(1-\varphi)}{M} \ln(1-\varphi) + \varphi(1-\varphi)\chi_{wp}, \quad (1.1)$$

describes the free energy of mixing of n_p moles of polymer liquid with n_w moles of the water solvent; $\beta = 1/kT$, φ is the solvent volume fraction, $M = \bar{v}_p/\bar{v}_w$ (the ratio of the molar volumes of the pure liquids) is the operational polymerization index, and χ_{wp} is the FH interaction coefficient. Here we study the concentration dependence of χ_{wp} , important for mixing the dissimilar liquids of water and chain molecules that have a non-trivial aqueous solubility. The FH model is routinely adopted for discussion of aqueous solutions of chain molecules of sub-polymeric length.³⁻⁵ The study below highlights direct access to the osmotic pressures of these solutions, and thus can address long-standing research on biophysical hydration forces.⁶

Though the traditional statistical mechanical calculation⁷ that arrives at Eq. (1.1) is not compelling for aqueous materials, the FH model captures two dominating points. Firstly, it identifies the volume fraction φ as the preferred concentration variable, associated with the physical assumption that the excess volume of mixing vanishes. This step partially avoids difficult statistical mechanical packing problems.⁸ Secondly, Eq. (1.1) captures the reduction of the chain molecule ideal entropy by the factor $1/M$. The physical identification of the polymerization index M as \bar{v}_p/\bar{v}_w as thermodynamically consistent as noted below, but is a crude description of the molecular structure of polymers. With these points recognized, however, the interaction contribution of Eq. (1.1) can be regarded

as an interpolation between the ends $\varphi = 0, 1$ of the composition range.

The simplest expectation⁷⁻¹⁰ for the interaction parameter is

$$\chi_{wp} \propto -\beta \left(a_{ww} - \frac{2a_{wp}}{M} + \frac{a_{pp}}{M^2} \right) \quad (1.2)$$

where the parameters $a_{\eta\nu}$ gauge the strength of dispersion interactions in van der Waals models of liquids.¹¹ That this justification is implausible for aqueous solutions¹² underscores the lack of a basic understanding of χ_{wp} for aqueous solutions.

The simple temperature dependence of Eq. (1.2) is a reasonable starting point, but aqueous solutions exhibit alternative temperature dependences of specific interest, hydrophobic effects.¹³ More troublesome, Eq. (1.2) does not depend on concentration, though experiments on the PEG/water system^{10,14} show substantial concentration dependence. Beyond that difficulty, those results exhibit a temperature trend opposite to Eq. (1.2), *i.e.*, stronger interactions at higher T consistent with the classic folklore of hydrophobic effects.¹⁰ In contrast, when the solvent is methanol¹⁵ the observed concentration dependence is less strong, though non-trivial and trending with concentration in the opposite direction from the aqueous solution results. The temperature dependences for the methanol case is qualitatively consistent with the simple expectation of Eq. (1.2). In further contrast, with ethanol as solvent¹⁶ the observed concentration dependence is distinctly modest.

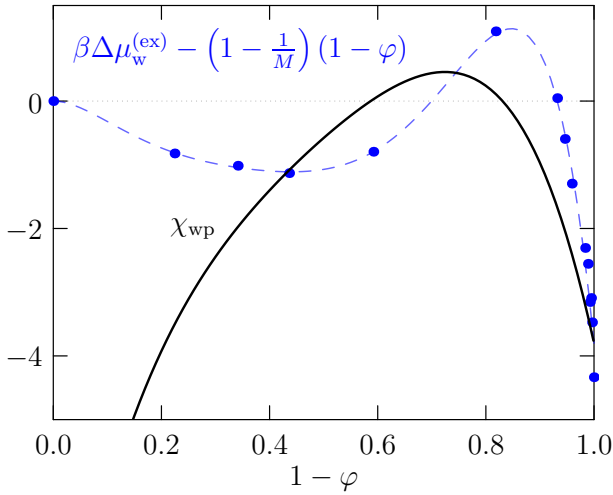


FIG. 1: Blue points and dashed curve: accumulated evaluation of Eq. (2.3). The solid curve is the implied $\chi_{\text{WP}}(\varphi)$.

II. THEORY

These puzzles may be addressed by analyzing the chemical potential of the water,¹⁰

$$\beta\Delta\mu_{\text{w}}^{(\text{ex})} = \left(1 - \frac{1}{M}\right)(1 - \varphi) + \frac{\partial(\varphi\chi_{\text{WP}})}{\partial\varphi}(1 - \varphi)^2, \quad (2.3)$$

where

$$\Delta\mu_{\text{w}}^{(\text{ex})} = \mu_{\text{w}}^{(\text{ex})}(\varphi, p, T) - \mu_{\text{w}}^{(\text{ex})}(\varphi = 1, p, T), \quad (2.4)$$

the interaction (or *excess*) contribution to the chemical potential of the water, referenced to the pure liquid value. The osmotic pressure π ,⁷

$$\beta\pi\bar{v}_{\text{w}} = -\ln\varphi - \beta\Delta\mu_{\text{w}}^{(\text{ex})}. \quad (2.5)$$

provides further perspective on $\Delta\mu_{\text{w}}^{(\text{ex})}$. Beyond assuming that the excess volume of mixing vanishes, Eq. (2.5) makes the standard approximation that the solvent is incompressible.¹⁷ To justify the identification $M = \bar{v}_{\text{p}}/\bar{v}_{\text{w}}$ noted above, we utilize Eq. (2.3), and expand through $(1 - \varphi)^2$ to obtain

$$\beta\pi V/n_{\text{p}} \sim 1 + \left(\frac{n_{\text{p}}}{V}\right)\bar{v}_{\text{w}}M^2\left(\frac{1}{2} - \hat{\chi}\right), \quad (2.6)$$

with $\bar{v}_{\text{w}}M^2\left(\frac{1}{2} - \hat{\chi}\right) = B_2$ thus the osmotic second virial coefficient. We adopt here the short-hand notation $\hat{\chi} = \partial(\varphi\chi_{\text{WP}})/\partial\varphi$. The identification of M in the contribution $(1 - \varphi)\left(1 - \frac{1}{M}\right)$ thus leads to the proper behavior in the ideal solution limit.

As suggested above, the intent of the FH model is that a concentration-independent χ_{WP} should describe the effects of enthalpic interactions. Our less-committal analysis acquires practical significance from

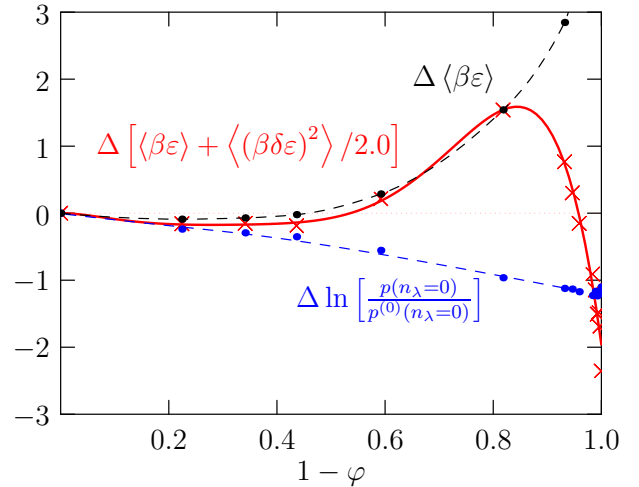


FIG. 2: ‘ Δ ’ indicates the difference from the pure solvent value, *i.e.*, $\Delta\langle\beta\varepsilon\rangle = \langle\beta\varepsilon\rangle(\varphi) - \langle\beta\varepsilon\rangle(\varphi = 1)$. A water molecule loses stabilizing outer-shell interactions through intermediate concentrations, and then regains favorable outer-shell contributions on the solvent-poor side of the concentration range. The dashed-blue curve shows the combined packing and chemical contributions.

recent development of molecular quasi-chemical theory for the excess chemical potential of the water in aqueous solutions.^{12,18,19} The central result

$$\beta\mu_{\text{w}}^{(\text{ex})}(\varphi, p, T) = -\ln p^{(0)}(n_{\lambda} = 0) + \ln\langle e^{\beta\varepsilon} | n_{\lambda} = 0 \rangle + \ln p(n_{\lambda} = 0) \quad (2.7)$$

is a physical description in terms of packing, outer-shell and chemical contributions, a comprehensive extension of a van der Waals picture.¹¹ The packing contribution is obtained from the observed probability $p^{(0)}(n_{\lambda} = 0)$ for successful random insertion of a spherical cavity of radius λ into the simulation cell. Similarly, the chemical contribution is defined with the probability $p(n_{\lambda} = 0)$ that a water molecule in the system has zero neighbors within the radius λ of its O atom. The outer-shell contribution is a partition function involving the binding energy ε , conditional on the inner-shell being empty. The condition permits a Gaussian statistical approximation,

$$\ln\langle e^{\beta\varepsilon} | n_{\lambda} = 0 \rangle \approx \beta\langle\varepsilon | n_{\lambda} = 0 \rangle + \beta^2\langle\delta\varepsilon^2 | n_{\lambda} = 0 \rangle/2, \quad (2.8)$$

involving the mean and variance of binding energies of molecules that have zero neighbors within radius λ .

With this background, we evaluate

$$\frac{\partial(\varphi\chi_{\text{WP}})}{\partial\varphi}(1 - \varphi)^2 = \beta\Delta\mu_{\text{w}}^{(\text{ex})} - \left(1 - \frac{1}{M}\right)(1 - \varphi). \quad (2.9)$$

Representing then

$$\frac{\partial(\varphi\chi_{\text{WP}})}{\partial\varphi} = \sum_{n=0} c_n (1-\varphi)^n, \quad (2.10)$$

and integrating, with $\varphi\chi_{\text{WP}} = 0$ at $\varphi = 0$, we obtain

$$\chi_{\text{WP}} = \sum_{n=0} \frac{c_n}{(n+1)\varphi} \left[1 - (1-\varphi)^{n+1} \right]. \quad (2.11)$$

III. RESULTS AND DISCUSSION

We thus analyze $\chi_{\text{WP}}(\varphi)$ for aqueous solutions for methyl-capped PEO oligomers²⁰ $\text{CH}_3(\text{CH}_2\text{-O-CH}_2)_{11}\text{CH}_3$ on the basis of accessible molecular simulation data.²¹ For this mixture we find $M = 27.6$, with the excess volumes of mixing similar to experimental results for similarly sized PEG 400:¹⁴ negative and small, though slightly larger than the comparable experimental case. The dielectric constant of these solution varies linearly with solvent volume fraction φ .

Eq. (2.7) is correct for any physical λ ,¹⁸ and we choose $\lambda = 0.29$ nm as a balance between statistical and systematic accuracy. The Gaussian approximation will be more accurate for larger λ . But the data set satisfying the condition $n_\lambda = 0$ gets smaller and the statistical accuracy is degraded with increasing λ . The latter point becomes more serious at lower water concentrations because fewer water molecules are present. Nevertheless, only the difference Eq. (2.4) is required, so systematic errors should be balanced to some extent.

Composing Eq. (2.3) produces a structured dependence on φ (FIG. 1). Extracting the individual quasi-chemical theory contributions (FIG. 2) shows that the distinctive variation with φ is due to the outer-shell (long-ranged) contributions: a water molecule loses stabilizing outer-shell interaction partners through intermediate concentrations, then regains favorable free energies through the fluctuation contribution of the Gaussian formula (Eq. (2.8)). These countervailing trends are not synchronous, so the net result is a non-monotonic function of φ .

The $\chi_{\text{WP}}(\varphi)$ (FIG. 3) describes separation of a water-poor solution from a water-rich phase. The osmotic pressure (FIG. 4) further characterizes the transition. To confirm the predicted phase separation, we simulated coexistence of water-rich and water-poor solutions (FIG. 3). The two fluids did indeed coexist stably on the simulation time scale of 20 ns, though the dynamics of the water-poor solution are distinctly sluggish: the self-diffusion coefficient of the water in the water-poor phase is about a 1/4th of that in the water-rich phase.

In assessing the coexisting water-poor phase, we note that these chains are short and the capping groups play a significant role. Comparable molecular-weight PEO chains with one hydroxyl and one methoxy termination are pastes at low water content. Methoxy terminated PEO chains as small as two-times larger than

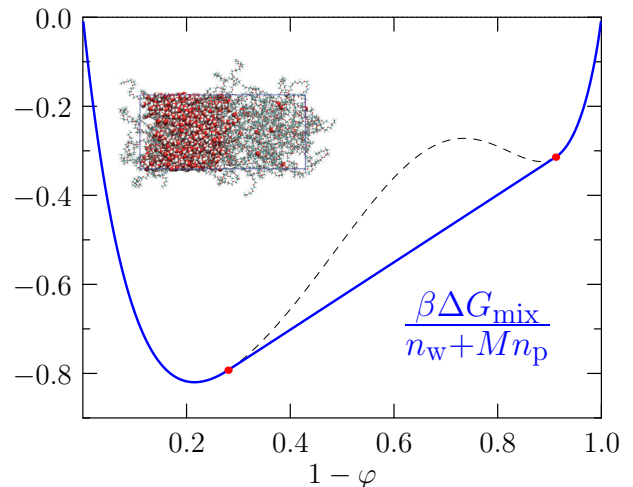


FIG. 3: Mixing free energy and double tangent construction. INSET: Coexisting phases with chain-molecule volume fraction $1 - \varphi \approx 0.34, 0.99$. This coexistence is stable on the simulation time scale of 20 ns.

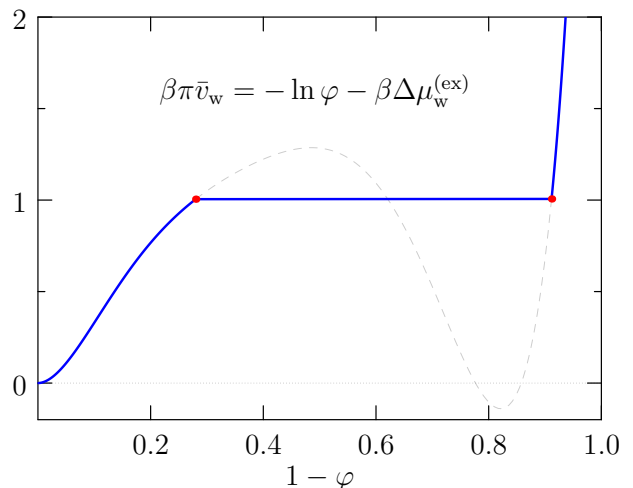


FIG. 4: Osmotic pressures, Eq. (2.5). The coexistence points identified in FIG. 3 have equal osmotic pressures, as they should. The osmotic second virial coefficient is positive.

the present case form crystals with Li electrolytes at these temperatures.²² The difference between the predicted coexistence points and the compositions exhibited in FIG. 3 might be due to the assumption of ideal volumes of mixing. Though the excess volumes are small, they are largest in the interesting intermediate concentration $1 - \varphi \approx 0.3$ region. This should receive further study.

IV. CONCLUSIONS

The observations here should help in formulating a defensible molecular theory of PEO (aq) phase transitions. The interesting $\chi_{wp}(\varphi)$ concentration dependence derives from long-ranged interactions.

This analysis provides straightforward predictions of osmotic pressures, not requiring detailed analysis of 2-body (or successive few-body) contributions. This realization should help in studies of osmotic stress.²³

V. ACKNOWLEDGEMENT

The financial support of the Gulf of Mexico Research Initiative (Consortium for Ocean Leadership Grant SA 12-05/GoMRI-002) is gratefully acknowledged. We thank S. J. Paddison for helpful conversations.

VI. METHODS

Parallel tempering simulations, implemented²¹ within GROMACS 4.5.3,²⁴ were used to enhance the sampling

at the $T = 300$ K temperature of interest. Parallel tempering swaps were attempted at a rate of 100/ns, which resulted in a success rates of 15-30%. The chain molecules were represented by the OPLS-aa force field,²⁵ and the SPC/E model was used for water.²⁶ Long-range electrostatic interactions were treated in standard periodic boundary conditions using the particle mesh Ewald method with a cutoff of 0.9 nm. The Nosé-Hoover thermostat maintained the constant temperature and chemical bonds involving hydrogen atoms were constrained by the LINCS algorithm. After energy minimization and density equilibration at 300.4 K and $p = 1$ atm, 40 replicas spanning 256-450 K, each at the same volume, were simulated for 10 ns. The pure liquid molar volumes were $\bar{v}_w = 0.0178$ dm³/mole, $\bar{v}_p = 0.490$ dm³/mole, so $M = 27.6$. Configurations of the $T = 300.4$ K replica were sampled every 0.5 ps for subsequent analysis. The packing, outer-shell and chemical terms were calculated separately using the replica at 300.4 K. 30,000 uniformly spaced trial insertions were used to estimate the packing term. The generalized reaction field method,²⁷ cutoff at 1 nm, was used to calculate the electrostatic contribution to the binding energies.

-
- ¹ Flory, P. J. *Principles of Polymer Chemistry*; Cornell University Press: Ithaca, 1953.
- ² Huggins, M. L. *J. Chem. Phys.* **1941**, *9*, 440.
- ³ Sharp, K. A.; Nicholls, A.; Fine, R. F.; Honig, B. *Science* **1991**, *252*, 106–109.
- ⁴ De Young, L. R.; Dill, K. A. *J. Phys. Chem* **1990**, *94*, 801–809.
- ⁵ Stillinger, F. H. *J. Chem. Phys.* **1983**, *78*, 4654–4661.
- ⁶ Parsegian, V.; Zemb, T. *Curr. Op. Coll. & Interface Sci.* **2011**, *16*, 618–624.
- ⁷ Hill, T. L. *An Introduction to Statistical Thermodynamics*; Addison-Wesley Publishing: Reading MA, 1960.
- ⁸ Beck, T. E.; Paulaitis, M. E.; Pratt, L. R. *Potential distribution theorem and statistical thermodynamics of molecular solutions*; Cambridge University Press: New York, 2006.
- ⁹ Doi, M. *Introduction to Polymer Physics*; Oxford University, 1995.
- ¹⁰ Bae, Y. C.; Shim, D. S., J. J. and Soane; Prausnitz, J. M. *J. Appl. Poly. Sci.* **1993**, *47*, 1193–1206.
- ¹¹ Chandler, D.; Weeks, J. D.; Andersen, H. C. *Science* **1983**, *220*, 787–794.
- ¹² Shah, J. K.; Asthagiri, D.; Pratt, L. R.; Paulaitis, M. E. *J. Chem. Phys.* **2007**, *127*, 144508 (1–7).
- ¹³ Pohorille, A.; Pratt, L. R. *Orig. Life Evol. Biosp.* **2012**, *42*, 405–409.
- ¹⁴ Eliassi, A.; Modarress, H. *J. Chem. & Eng. Data* **1999**, *44*, 52–55.
- ¹⁵ Zafarani-Moattar, M. T.; Tohidifar, N. *J. Chem. & Eng. Data* **2006**, *51*, 1769–1774.
- ¹⁶ Zafarani-Moattar, M. T.; Tohidifar, N. *J. Chem. & Eng. Data* **2008**, *53*, 785–793.
- ¹⁷ Kirkwood, J. G.; Oppenheim, I. *Chemical Thermodynamics*; McGraw-Hill: New York, 1961.
- ¹⁸ Paliwal, A.; Asthagiri, D.; Pratt, L. R.; Ashbaugh, H. S.; Paulaitis, M. E. *J. Chem. Phys.* **2006**, *124*, 224502.
- ¹⁹ Chempath, S.; Pratt, L. R.; Paulaitis, M. E. *J. Chem. Phys.* **2009**, *130*, 054113(1–5).
- ²⁰ Chaudhari, M. I.; Pratt, L. R.; Paulaitis, M. E. *J. Chem. Phys.* **2010**, *133*, 231102.
- ²¹ Chaudhari, M. I. Molecular simulations to study thermodynamics of polyethylene oxide solutions. Ph.D. thesis, Tulane University, 2014.
- ²² Gadjourova, Z.; Andreev, Y. G.; Tunstall, D. P.; Bruce, P. G. *Nature* **2001**, *412*, 520–523.
- ²³ Cohen, J. A.; Podgornik, R.; Hansen, P. L.; Parsegian, V. A. *J. Phys. Chem. B* **2009**, *113*, 3709–3714.
- ²⁴ van der Spoel, D.; Lindahl, E.; Hess, B.; Groenhof, G.; Mark, A. E.; Berendsen, H. J. C. *J. Comp. Chem.* **2005**, *26*, 1701–1718.
- ²⁵ Jorgensen, W. L.; Maxwell, D. S.; Tirado-Rives, J. *J. Am. Chem. Soc.* **1996**, *118*, 11225–11236.
- ²⁶ Berendsen, H. J. C.; Grigera, J. R.; Straatsma, T. P. *J. Phys. Chem.* **1987**, *91*, 6269–6271.
- ²⁷ Tironi, I. G.; Sperb, R.; Smith, P. E.; van Gunsteren, W. F. *J. Chem. Phys.* **1995**, *102*, 5451.